SPE 125329

Fracture Characterizing and Modeling of a Porous Fractured Carbonate Reservoir

Rouhollah Dashti, University of Tehran; Mohammad Bagher Bagheri, Sharif University of Technology; and Shahzad Ulhaq, WSI

This paper was prepared for presentation at the 2009 SPE/EAGE Reservoir Characterization and Simulation Conference held in Abu Dhabi, UAE, 19–21 October 2009.

Abstract

Anisotropy and heterogeneity in reservoir properties introduce challenges during the development of hydrocarbon reservoirs in naturally fractured reservoirs. In reservoir simulations, grid-block properties are frequently assigned to obtain reasonable history matches. Even then, accuracy with regard to some aspects of the performance such as water or gas cuts, breakthrough times, and sweep efficiencies may be inadequate. In some cases, this could be caused by the presence of substantial flow through natural fractures.

In this work the fracture characterization and modeling was performed in a highly fractured carbonate reservoir in SW Iran. It was observed that reservoir simulation based on the generated fracture model present a more reasonable history matching of the production. The study indicates that NE-SW is the dominant orientation of critically stressed fractures that are most problematic for gas/water breakthrough.

The primary objectives of this study are: a) construct a fracture 3D model to be used in reservoir simulation and b) distinguish the most problematic fractures in water/gas breakthrough. The steps of this study are as follows:
-Constructing the 3D geological framework of the reservoir.
-Identifying and characterizing natural fractures at the well level using borehole images.
-Generating the 3D-stochastic model of discrete fracture network (DFN), incorporating image log data with outcrop analogies studies in the context of buckle folding mechanism.
-Scaling up the fracture model with integration of well test results
-Running reservoir simulation based on the scaled-up fracture model to validate the model and observe the history matching
-Performing critically stressed fractures (CSF) analysis to distinguish problematic fractures.

Introduction

Naturally fractured reservoirs (NFRs) comprise a large portion of carbonate reservoirs in Middle East. Numerous challenges dealing with fracture system behavior incorporated with natural complexity of carbonates present a challenging environment for geoscientists and reservoir engineers to characterize and predict such reservoirs. However, conventional dual porosity simulations of fractured reservoirs are usually based on frequently assigning values to fracture properties to obtain reasonable history match for production of the field. This creates a big source of uncertainty in predicting the reservoir behavior and often results in frequent surprises during development. Comprehensive characterization coupled with modeling of fracture network is the key for understanding the performance of NRFs in particular carbonates ones.

In the present study, the globally well-known fractured reservoir of Asmari in a field in Zagros fold belt was characterized for the natural fractures to develop a comprehensive model of fracture network in a 3D modeling software using stochastic DFN method. This model then was used as input into the reservoir simulator to run a dual porosity model. elaborate the problem of gas and water breakthrough. Shortage of data e.g. quality seismic data was the main challenge in building the fracture model. An extensive investigation of outcrops and other source of information on natural fractures and structural style of Asmari formation were performed to develop the optimized model using Discrete Fracture Network (DFN) method.

Reservoir stratigraphy

The Asmari Formation is an Oligocene-Early Miocene age platform carbonate with occasional occurrence of sandstones (Ahwaz member). It is the most prolific oil reservoir in Iran and, moreover, it is commonly regarded as one of the classic fractured carbonates in the world, with production rates strongly influenced by the presence, or not, of fractures [3], [11], [12].

In the study field, Asmari formation comprise of mainly dolomite and occasionally limestone with low clay content. The porosity of the matrix is relatively high (10-30%) in contrast to many other fracture reservoirs in the region. This distinctively high porosity can be due to secondary dolomitization of initial limetones. Asmari carbonates are constrained by two evaporite units: Gachsaran at top and Kalhur member at below. In general Asmari formation in the study area shows little lithological heterogeneity (Figure 1).

Methodology and Workflow

The available well data set was borehole image logs in 4 wells (A to D), conventional logs, well-test results, production logs, production history, formation pressure tests and graphic well logs. In addition to these well data, underground contour map (UGC) of the field and stratigraphic well tops were available. The only available seismic data was an old low quality 2D seismic, which could not be used in the project. Instead, great help was obtained from extensive fracture studies on Asmari outcrops in nearby areas. The main steps of the study are summarized as follows:

- Data set was gathered, quality checked and organized
- Study of the tectonic and structural style of the anticline
- Building the 3D structural and stratigraphic model of the field in the modeling software
- Processing the borehole image logs along with conventional logs
- Identifying and characterizing natural and induced fractures on borehole image logs
- Computing fracture attributes (density, porosity and aperture) of open fractures
- Determining and classifying the main fracture sets and computing the fracture intensity of each set
- Generating the main fracture drivers grids including curvature, distance to fold axis and reciprocal to dip angle
- Building the discrete fracture network and the required fracture attributes grids i.e. fracture aperture, length and permeability maps
- Upscaling the DFN model and running reservoir simulation.

In the next phase of the study, we used critically stressed fractures analysis (CSFA) to elaborate the fracture patterns and in-situ stresses in relation to water and gas breakthroughs to determine main problematic fracture set(s).

Tectonic, fold geometry and mechanical stratigraphy

The Zagros mountain chain including the Dezful Embayment represents the northeastern part of the Arabian Plate. The Zagros developed as a result of plate convergence, particularly during the Late Miocene-Pliocene orogenic phase (Hessami et al. 2001). The anticlines at reservoir level (Asmari Formations and below) in this area are in general asymmetric with a steep SW limb. The Zagros fold belt is often cited as one of the best examples of large-scale buckle folding [8]. Satellite images and aerial photographs show numerous examples of anticlines with aspect ratios (half wavelength to axial length ratio) of between 5:1 and 10:1, which are typical of buckle folds on all scales and which display the characteristic en echelon spatial organization in plan view [2].

The study field is an asymmetric anticline with NW-SE fold axis strike located in Zagros (simply) folded belt (Figure 2) .It has an aspect ratio of 5:1 with cylindrical shape and plunges at both ends. In fact, it is a typical example of buckle folds in the region referred to as periclines [8]. Determination of fold types plays a major role in

3D modeling of the fracture network since the mechanism and type of the fold controls the fracture patterns expected and their distribution in subsurface structure.

Asmari carbonates as a competent unit are bounded by two incompetent units, Gachsaran formation and Kalhur member in the study field. Open hole logs along with graphic well logs show that Asmari consist of moderately uniform dolomitic beds as the dominant lithology with low shale content. This relative homogeneity of the reservoir is considered as an important factor of quite large vertical extent of fractures.

Identifying and characterizing fractures using borehole images

Image logs recorded in 4 wells were processed and interpreted using a uniform scheme developed for this field. Almost all of the identified fractures were appeared as conductive features on borehole images, which is due to conductive mud filled the fractures. These fractures are classified as open natural fractures. Most of the fractures created continuous trace on image logs, while the rest had discontinuous traces. A few number of resistive or closed fractured were also detected, which were not considered in this study as they do not have major impact on reservoir behavior. Dip and azimuth of the open fractures were analyzed and majority of them found to be high angle fractures. Fracture attributes of these including density, aperture and porosity were also computed in each well. Most of the open fractures had aperture between 0.1 mm to 0.2 mm and porosity of less than 0.2% (Figure 4). The fact that almost all fractures are open can imply that fracturing of the reservoir should have occurred after pervasive dolomitization of the formation. Otherwise, dolomitizing fluids, which are usually mineral saturated could have healed many of the pre-existing fractures.

Fracture sets classification and fracture intensity

Based on image analysis results, fractures in the studied field can be classified as a network of systematic fractures with no major faults. This occurrence and dip attributes of the fractures had a perfect match with expected fracture system of a typical buckle fold in Zagros studied and defined by a number of workers mainly on outcrops of the Asmari formation in the area of Zagros fold belt e.g. McQuillan 1974 and 2007, Wennberg 2007, Sangree 1968, Halsey and Corrigan (1977) etc (Figure 3). This offer great help to define the distribution of natural fractures and propagate these fractures across the field. According to outcrop studies there are 4 main fracture patterns present in majority of periclinal structures in the region: Parallel-axial and cross-axial (type II and I, Stearns 1968) (Figure 3) the two dominant fold related fracture patterns along with N-S and E-W fractures related to basement faulting.

Based on the dip and strike statistical analysis, we defined four fracture sets correlating to major fracture types explained above: Set-1 with NW-SE trend, set-2 with NE-SW, set-3 with N-S trend and set-4 with E-W trend. Fracture set-1 is called longitudinal fractures, as their strike is almost parallel to the strike of the bedding. Fracture set-2 is called transverse fractures, as their strike is approximately perpendicular to bedding. Fracture sets 3&4 are oblique fractures having angular relationship with bedding strike (Figure 5).

Fracture intensity is the property of interest for modeling, and will be upscaled and used as the basic data for creation of the fracture network (DFN). Creating a fracture intensity log is a process of taking discrete observation and transforming them to statistical values, which describe the fracture distribution. These fracture intensity logs at well level then should be incorporated with appropriate fracture drivers using neural network technique to generate fracture intensity map across the field. Fracture driver by definition is a property in the entire grid that could give us some additional info on the lateral extent of fractures. Identifying the best fracture drivers is a crucial step in fracture modeling and requires an adequate knowledge of the structure under study and the main controls on fracturing.

We computed fracture intensity for each individual fracture set in all four wells and incorporate them with fracture drivers of Structural curvature, distance to fold axis and reciprocal dip angle to generate fracture intensity maps. These drivers were identified and generated based on theoretical distribution model of buckle-fold fracture pattern [2] and more importantly real experiences in outcrop studies [3], [4].

Construction of the DFN model

To predict hydraulic behavior of the fracture network, we first built discrete fracture network (DFN) using commercial vendor software. We then used the same software to upscale the resulted DFN computing the directional permeabilities and matrix-fracture coupling parameter (σ). In a DFN model, a virtual rock volume is stochastically populated with planar objects representing natural fractures. The virtual fractures are assigned properties from statistical distributions defined by integration of outcrop and subsurface data, field production data and theories of mechanical and hydraulic behavior.

One of the critical parameters computed in DFN building was fracture permeability. However, as the fracture permeability is entirely dependent on fracture aperture, the aperture must have already been computed and statistically propagated in the 3D grid. To validate the aperture model in DFN, we crosscheck the results with the modeled aperture, which had been directly computed from image logs.

Fracture permeability in DFN was calculated using the technique described in IPTC 11971 [17]:

$$kh_{average} = \sum_{matrix}^{m=1...i} k_m h_m + \sum_{fracture}^{f=1...i} k_f h_f \quad \ldots\ldots[1]$$

Where kh is the factor resulted from pressure transient testing. Km and hm are permeability and block size of the matrix and Kf and hf are of fractures. Km can be obtained from core analysis and hm is calculated in refer to fracture spacing. Fracture height of hf is considered as cumulative fracture aperture in each well as interpreted from image logs. $Kh_{average}$ is the output of well test analysis (Figure 5).

Upscaling the DFN model

The DFN model is upscaled into the 3D geological model grid to give fracture porosity, permeability tensors (in the I, J and K grid directions) and a sigma factor property (connectivity between fractures and matrix) in each direction. Primary matrix porosity, permeability grids are already stored in the 3D geological model. These will be the input to a dual porosity simulation.

Noticeably high values of vertical permeability computed were a key observation in this stage. This is in contrast to what conventionally believed and is usually underestimated in simulation of fractured reservoirs. High values of vertical permeability, which is the result of high angle open fractures in the studied field, can be considered as one of the primary causes of early water and gas breakthrough (Figure 6).

Reservoir simulation

In reservoir simulations, fracture permeability and sigma factor are the main input parameters in dynamic fracture models. σ is the factor to account for the matrix-fracture interface area per unit volume (Eq. 1).

$$\sigma = 4\left[1/L_x^2 + 1/L_y^2 + 1/L_z^2\right] \quad \ldots\ldots[2]$$

Where, l_x, l_y and l_z are typical X, Y and Z dimensions of the matrix blocks in a relationship proposed by Kazemi (SPEJ Dec 76, 317-326). The dimensions of the matrix blocks used above are not the dimensions of the simulation grid, but of the elements of matrix material in the reservoir.
Although, well test analysis provides average values for permeability, but using these values for determining fracture permeability is not well understood. Therefore, in reservoir simulation, the model initialization for fracture permeability and sigma is usually based on initial guess, not reliable calculations and fracture properties are considered as matching parameters during field history matching. This usually impacts the simulation results for predicting reservoir dynamic behavior and fails to forecast the early breakthrough problems.

In this section we used two different 3D Geological models for dynamic simulation. The first one includes the fracture modeling and the distribution for the Sigma and fracture permeability and the other one dose not include the fracture modeling and a constant value has been considered for sigma as well as a constant multiplier for the fracture permeability based on matrix permeability.

The depth values of the gas-oil-contact as well as the oil-water contact at current condition were measured with formation tests in two wells. From those measurements it was estimated that the oil rim thickness is slightly more than 40m. The overview of the field at the beginning of its history including the fluid saturation is shown in Figure 7.

The major parameters, which have been investigated In order to compare two above, mentioned models are: production rate, static pressure measurements and oil rim thickness. Figure 8 through Figure 10 show the production comparison of these two models. Figure 11 shows the comparison between well bottom hole pressures at two different models. As it can be seen in this figure the pressure match with considering fracture modeling is relatively better. Figure 12 shows the oil rim thickness at the end of history at both models. The major observation is that, in the model with considering fracture modeling the oil saturation is less than the other model.

Critically-stressed fractures analysis to understand breakthrough problems

Understanding the water and gas breakthrough in the studied field was one of the primary objectives of this work. Initial investigations showed that these problems are due to presence of natural fractures. Critically stressed fracture analysis was carried out to recognize the most problematic fractures.

The concept of critically stressed fracturing is well described by C.Barton 1997 [14]. A natural fracture is considered to be critically stressed if the ratio of shear to normal stresses acting on the fracture surface exceeds the frictional strength of the reservoir rock. Barton et al verified that fluid flow in fractured rocks is largely controlled by critically stressed fractures (Figure 14). Critically stressed fracture analysis (CSFA) consists of the following activities:

- Characterization and identification of the orientation of the natural fractures.
- Estimation of magnitude and direction of the three principal in-situ stresses acting in the reservoir.
- Projection of the far field in-situ stress tensor onto the fracture planes to calculate the normal and shear stresses acting on each plane.
- Comparison of the stresses, plotted on a normalized Mohr-Coulomb diagram, and compared to the fracture shear failure envelope.
- Classification of the fractures as critically stressed if the ratio of shear to normal stress exceeds the shear failure fracture envelope.

- In-situ stresses and dominant stress regime

The drilling of borehole creates a stress disturbance around the borehole due to removal of the stress-bearing material that previously existed at that location. When the elevated stress around the borehole exceeds the strength of the rock, failure will occur and the borehole geometry will be altered. In particular, if the compressive stress around the borehole exceeds the compressive strength of the rock, borehole breakout will occur. Similarly, if the tensile stress exceeds the tensile strength of the rock, an induced fracture will occur. Failure at the borehole wall is therefore an indicator of the imbalance between the locally concentrated stress and strength of the rock.

Borehole images in 4 wells of this study were interpreted to capture the borehole breakout and induced fractures directions and distributions. The direction of induced fractures computed to be predominantly towards NE-SW, which can also be considered as the direction of maximum horizontal stress (σH). On the other hand, borehole breakout identified on images found to show the general NW-SE direction, which is the direction of minimum horizontal stress. These results then were used in professional software to compute the dominant stress regime of the field at the level of Asmari reservoir (Figure 13). Therefore, the in-situ stress tensor is defined as a strike-slip close to normal regime.

$$\sigma_{H,\max} \geq \sigma_v > \sigma_{h,\min} \quad \text{[3]}$$

Magnitude of vertical stress or overburden stress was computed by the following equation:

$$\sigma_v = \int_{sur}^{td} \rho_b g dz \quad \text{[4]}$$

As density log (ρ_b) was not available up to the surface, the densities of shallow formations were estimated from acoustic velocities.

For estimation of horizontal stresses the poroselastic equation introduced by Biot was used:

$$\sigma_h = \frac{v}{1-v}\sigma_v + \frac{1-2v}{1-v}\alpha P_p + \frac{E}{1-v^2}\varepsilon_x + \frac{vE}{1-v^2}\varepsilon_y \quad \text{[5]}$$

$$\sigma_h = \frac{v}{1-v}\sigma_v + \frac{1-2v}{1-v}\alpha P_p + \frac{E}{1-v^2}\varepsilon_y + \frac{vE}{1-v^2}\varepsilon_x \quad \text{[6]}$$

Formation pore pressure is required to compute the magnitude of effective stresses. This was obtained from pressure tests acquired in each of four wells under the study.

$$\sigma_{eff} = \sigma - P_p \quad (7)$$

- Friction angle and shear failure strength

Critically stressed fractures are almost independent of rock properties other than the shear failure and the Biot poroelastic parameter. Typically, the friction angle used for CSFA is around 30° based on extensive experimental tests made by Byerlee in 1978 [19]. However, according to Risnes 2008, friction angle has a decreasing trend as a function of increasing porosity and it can be in the range of 10° to 30°. As the Asmari reservoir in our case was a highly porous dolomite, after several sensitivity simulations, a friction angle of 20° was obtained experimentally for CSFA in this study.

- Critically stressed fracture analysis (CSFA) results

Critically stressed fractures can be identified once normal and shear stress components are plotted on a Mohr-Coulomb diagram and compared to the shear friction failure coefficient of fractures. The natural fractures would then be critically stressed if their shear to normal stress ratio were higher than the shear friction strength line.

This analysis was carried out for all four wells in this study. It was found that the fractures striking NE-SW and dip inclination of more than 60 degrees are critically stressed (Figure 14). These fractures are considered as the most efficient fluid flow pathways and in our case the most problematic features for water and gas breakthroughs. Distribution of such fractures were determined in three wells A, B and C and compared to production performance of these wells. In well B, where critically stressed fractures are more concentrated in lower part of the reservoir within the water zone, the well encountered early high water cut. While in well A, where such fractures are identified allover the reservoir, it suffers both water and gas breakthroughs and has to be almost abandoned. On the other hand, in well C, where critically stressed fractures have the least occurrence no major breakthrough issues have been faced yet (Figure 14).

In field scale, once the area of concentration of critically stressed fractures was compared with the region of high water and gas production, a reasonably good match were found, which also shows that these fractures are most problematic in this matter.

Conclusion

1. Developing 3D fracture model and acquiring spatial distribution of fracture static and dynamic properties result in more realistic simulation of naturally fractured reservoirs particularly in conning problems. DFN method offers the most efficient procedure to actualize the fracture network and its characteristics.

2. Outcrop studies provide a robust source of information about fracture system specification and distribution e.g. dominant fracture types, spatial occurrence relative to structural position, fracture length and height.

3. The sigma factor is an important parameter in dynamic simulation of the reservoir, lacking accurate estimation of that causes the dynamic model not to be match reliably in case of dual porosity models. The effect of considering sigma factor distribution is more sensible around gas oil contact rather than water oil contact.

4. Vertical permeability is computed to be high in the fracture model. This is due to presence of high angle fractures. Underestimation of this permeability can be a source of erroneous results in simulation. In this study this high vertical permeability can be a reason to facilitate water and gas breakthroughs.

5. Critically stressed fracture analysis was performed to identify the most problematic fractures in early water and gas breakthroughs. We concluded that NE-SW striking fractures with dip inclination of more than 60 degrees are potential critically stressed. In further development of the field these fracture should be avoided.

Acknowledgement

The authors would like to appreciate Mr. Ahmadreza Y.Sinaki (University of Curtin) for his support on this study.

References

1. Colman-Sadd, S.P., Fold Development In Zagros Simply Folded Belt, Southwest Iran, AAPG, V. 62. No. 6 (June 1978).

2. Cosgrove, J.W. and Ameen, M.S., A comparison of the geometry, spatial organization and fracture patterns associated with forced folds and buckle folds, Geological society, London, 2003.

3. McQuillan, H., Fracture Patterns on Kuh-e Asmari Anticline, Southwest Iran, AAPG, V. 58, No. 2 (February 1974).

4. Wennberg, O.P. and Azizzadeh, M., The Khaviz Anticline: an outcrop analogue to giant fractured Asmari Formation reservoirs in SW Iran, Geological society, London, 2007.

5. Stephenson, B.J. and Koopman, A., Structural and stratigraphic controls on fold-related fracturing in the Zagros Mountains, Iran: implications for reservoir development, Geological society, London, 2006.

6. Sepehr, M. and Cosgrove, J.W., Structural framework of the Zagros Fold–Thrust Belt, Iran, Marine and Petroleum Geology 21 (2004) 829–843

7. Blanc, E.J.P., Allen, M.B., Inger, S. and Hassani, H., Structural styles in the Zagros Simple Folded Zone, Iran, Journal of the Geological Society, London, Vol. 160, 2003

8. Sattarzadeh, Y., Cosgrove, J.W. and Vita-Finzi, C., The geometry of structures in the Zagros cover rocks and its neotectonic implications, Geological society, London, 2002.

9. Sattarzadeh, Y., Cosgrove, J.W. and Vita-Finzi, C., The interplay of faulting and folding during the evolution of the Zagros deformation belt, Geological society, London, 2000.

10. McQuarrie, N., Crustal scale geometry of the Zagros fold–thrust belt, Iran, Journal of Structural Geology 26 (2004) 519–535

11. Cedric, E., and Warman, H.R., Asmari oil fields of Iran, AAPG, 1970.

12. Beydoun, Z.R., Stoneley, R., Petroleum in the Zagros basin: a late tertiary foreland basin overprinted onto the outer edge of a vast hydrocarbon-rich Paleozoic-Mesozoic passive margin shelf, AAPG, 1992.

13. Nelson, R., Geologic Analysis of Naturally Fractured Reservoirs, 2001.

14. Barton, C., Zoback, M.D., Fracture permeability and its relationship to in-situ stress in the Dixie valley, Nevada, geothermal reservoir, Twenty-Second Workshop on Geothermal Reservoir Engineering, 1997.

15. Makel, G.H., The modeling of fractured reservoirs: constraints and potential for fracture network geometry and hydraulics analysis, Geological society, London, 2007.

16. Ameen, M.S., Fracture and in-situ stress characterization of hydrocarbon reservoirs: definition and introduction, Geological society, London, 2003.

17. Bahrami, H., Siavoshi, J., Characterization of fracture dynamic parameters to simulate naturally fractured reservoirs, IPTC 11971, 2008.

18. Verma, N.K., Franquent, A.J., Critically stressed fracture analysis in naturally fractured carbonate reservoirs-a case study in west Kuwait, SPE 105356, 2007.

19. Byerlee, J.D., The friction of rocks, Pure Appl. Geophy., 116, 615-629, 1978.

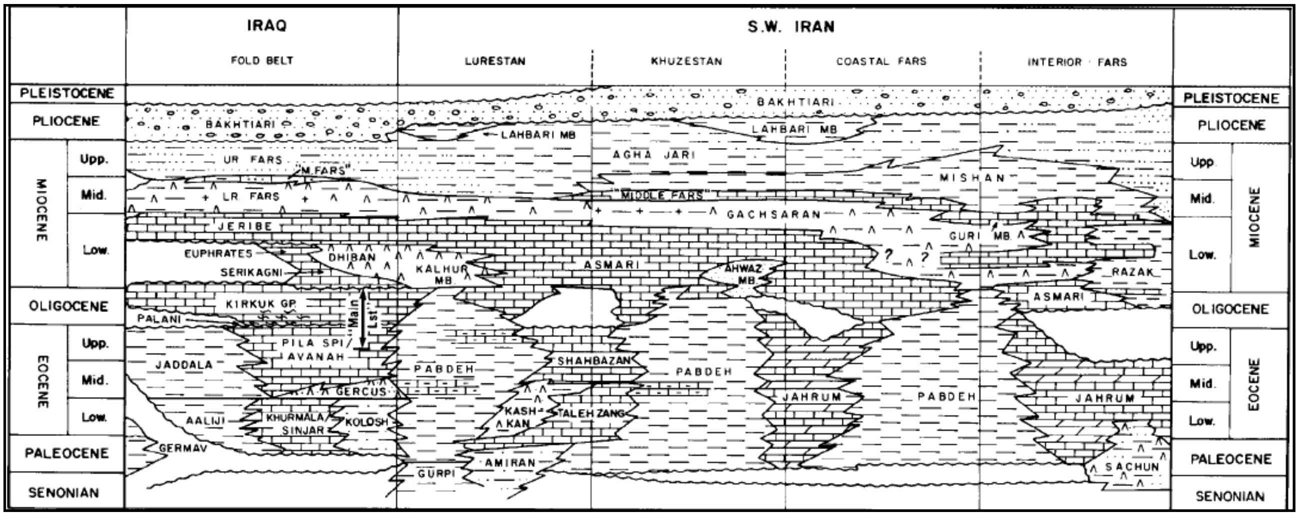

Figure 1: Stratigraphic column and the lithological and structural divisions of the Zagros Mountain Belt (Beydoun 1992).

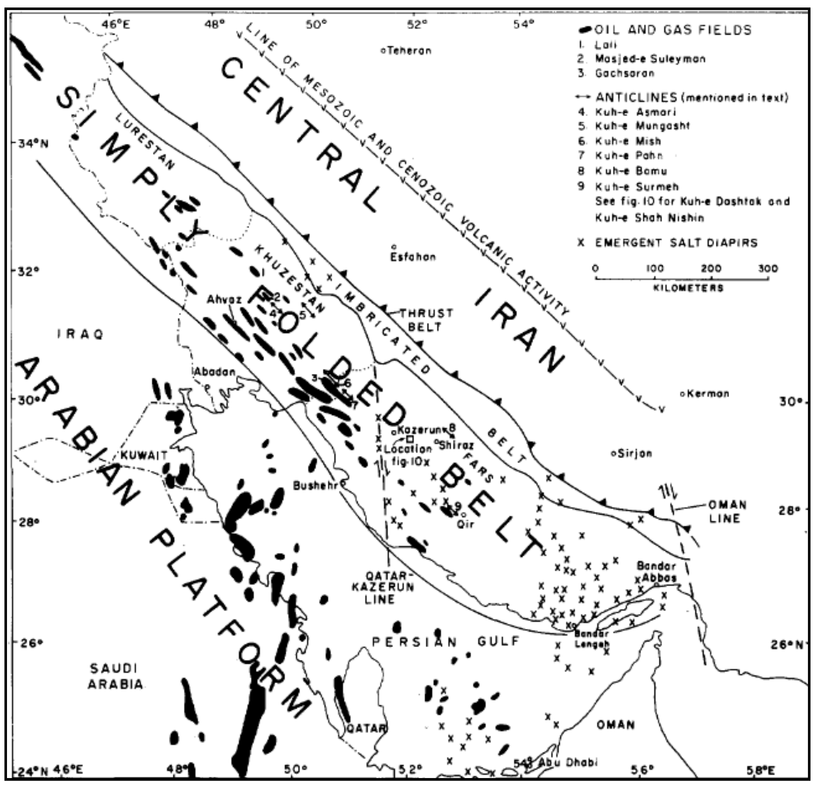

Figure 2: Zagros fold belt and oil field in SW Iran and Persian Gulf (Colman –Sadd 1978)

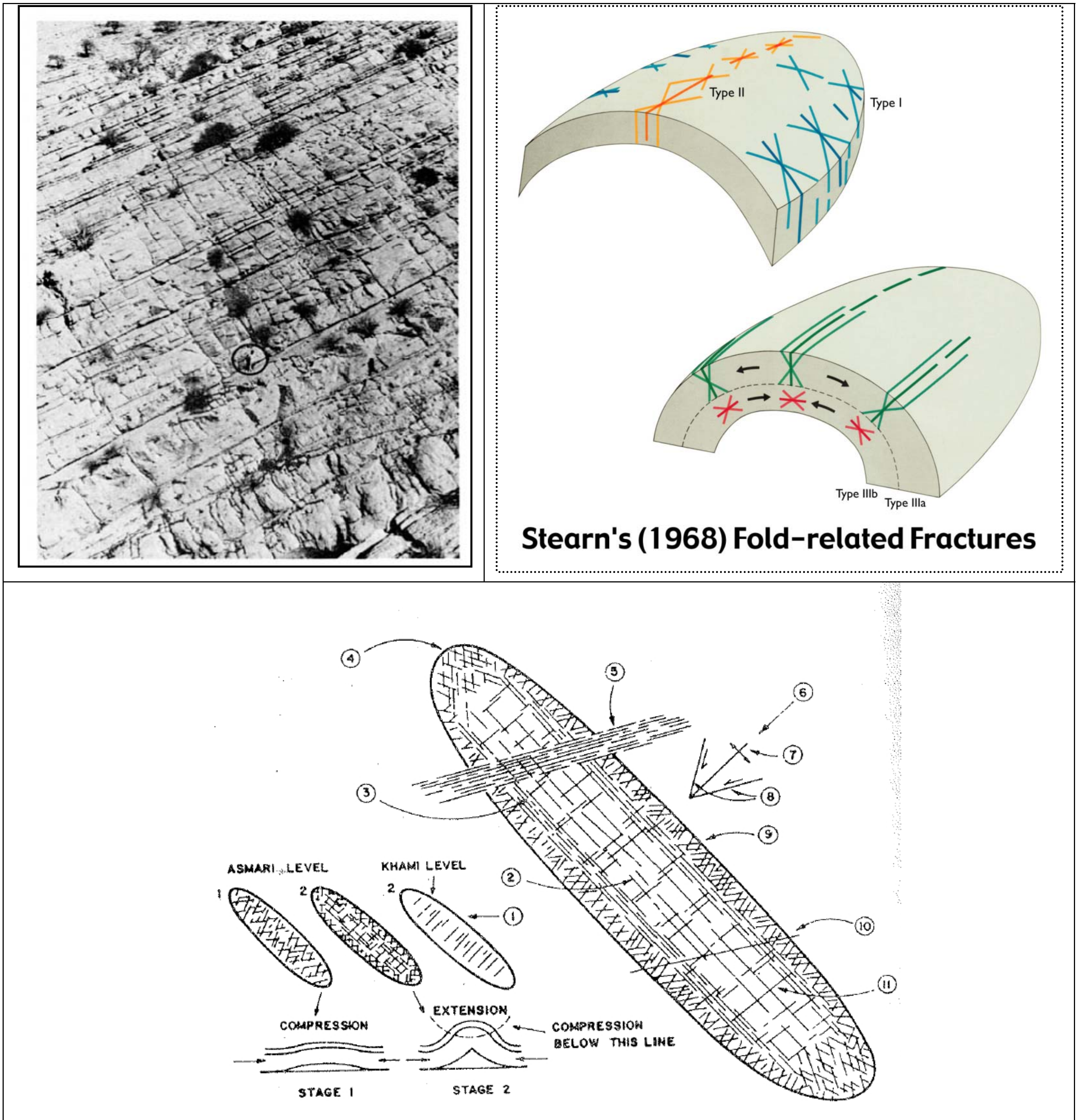

Figure 3: Above-Right, fold related fractures of Streans (1968), Above-left, Example of Asmari fractures in outcrop by McQuillan 1973. Below, ideal fracture system of a Zagros anticline, Moteie 1993.

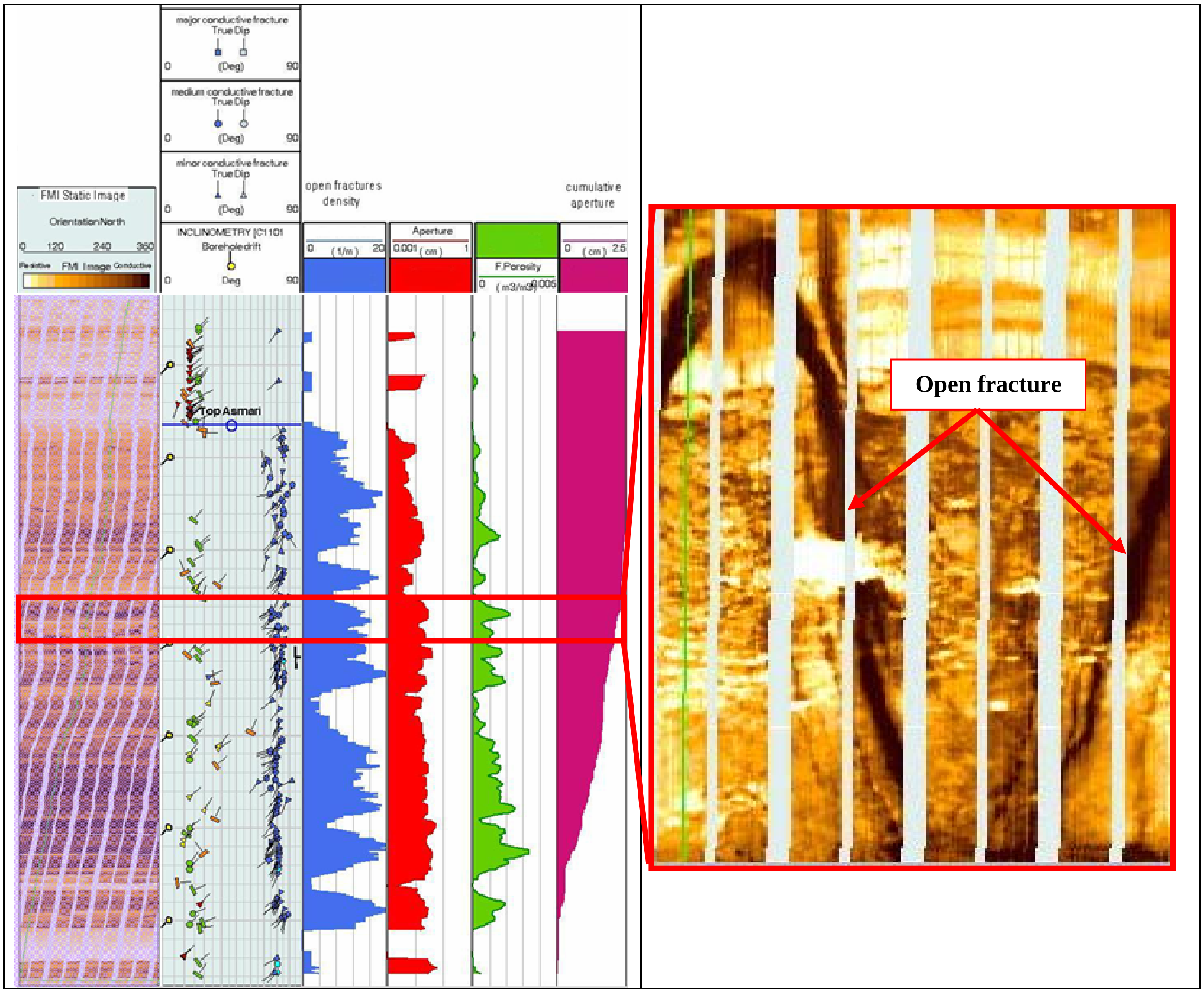

Figure 4: Fracture analysis summary in well-C with a snapshot of a large open fracture

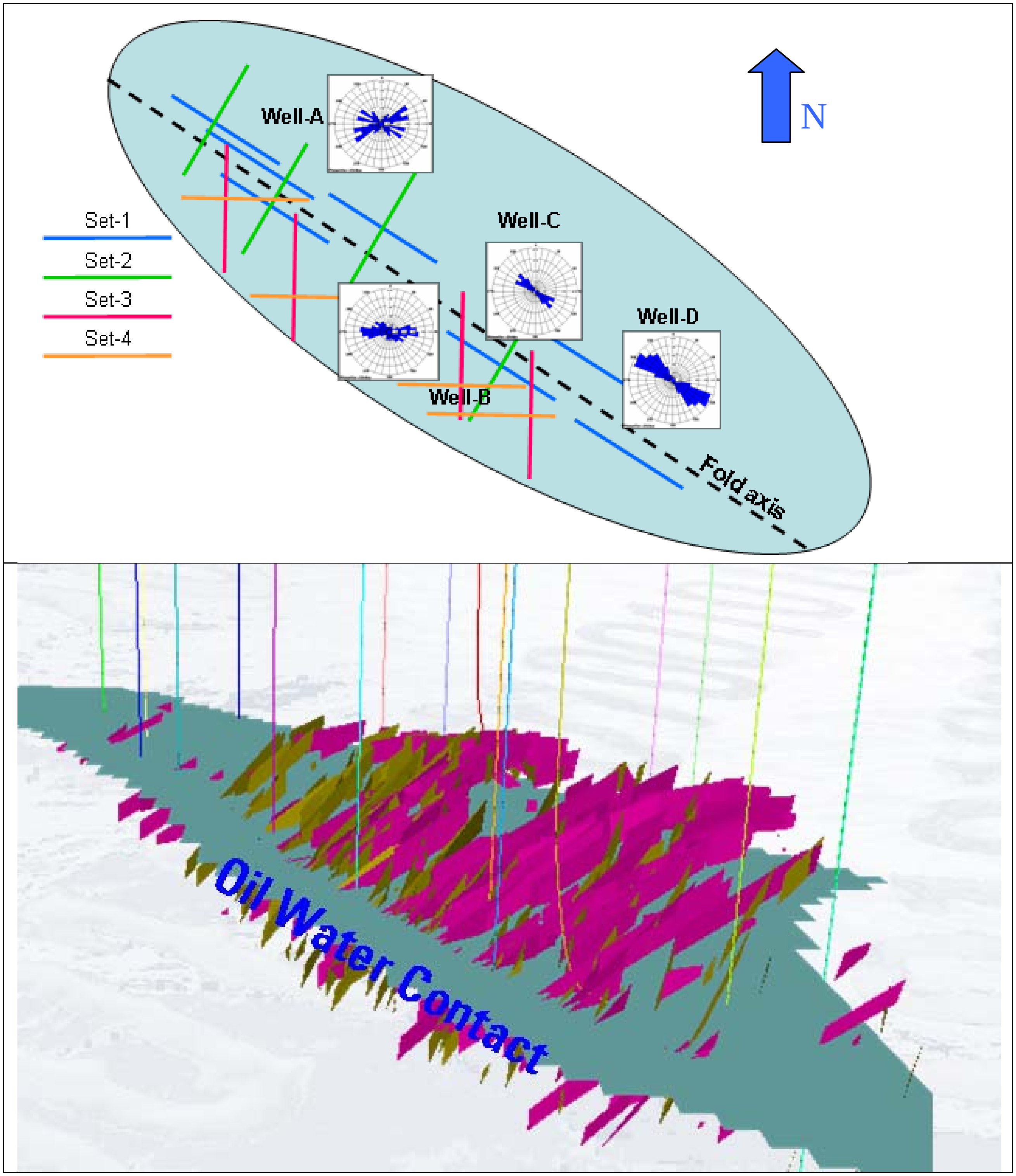

Figure 5: Above, strike diagram of natural fractures in the wells and the fracture sets shown on the schematic of the field. Below, DFN model of the reservoir

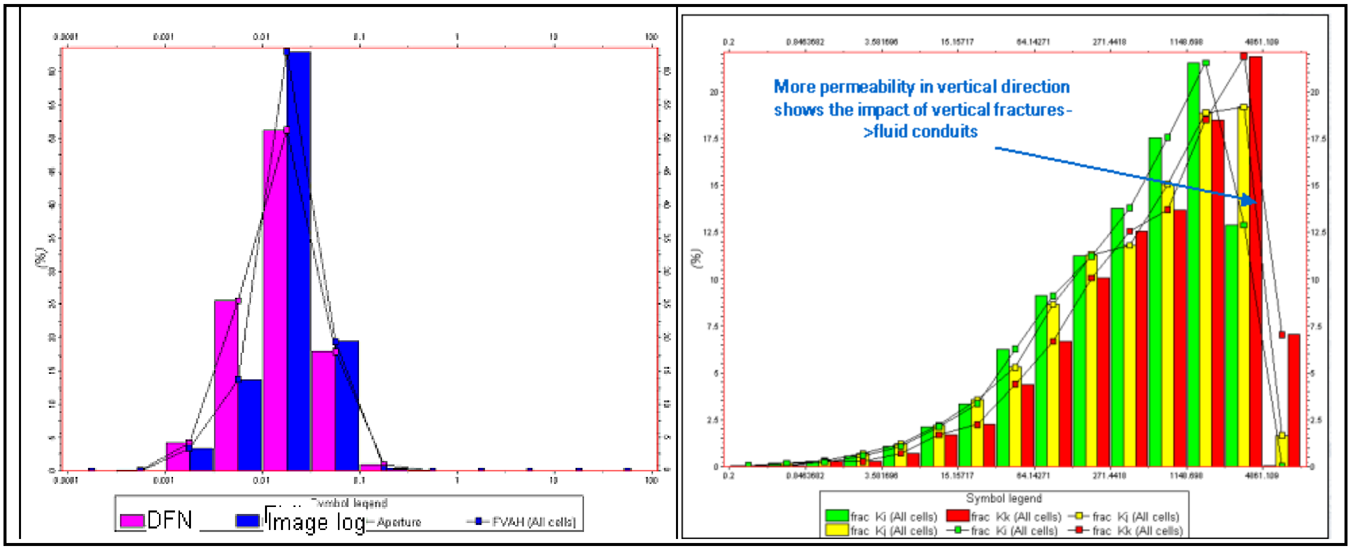

Figure 6: Left, fracture aperture computed and modeled from image logs and DFN, right, fracture permeabilities in three directions (red is Kf in vertical direction).

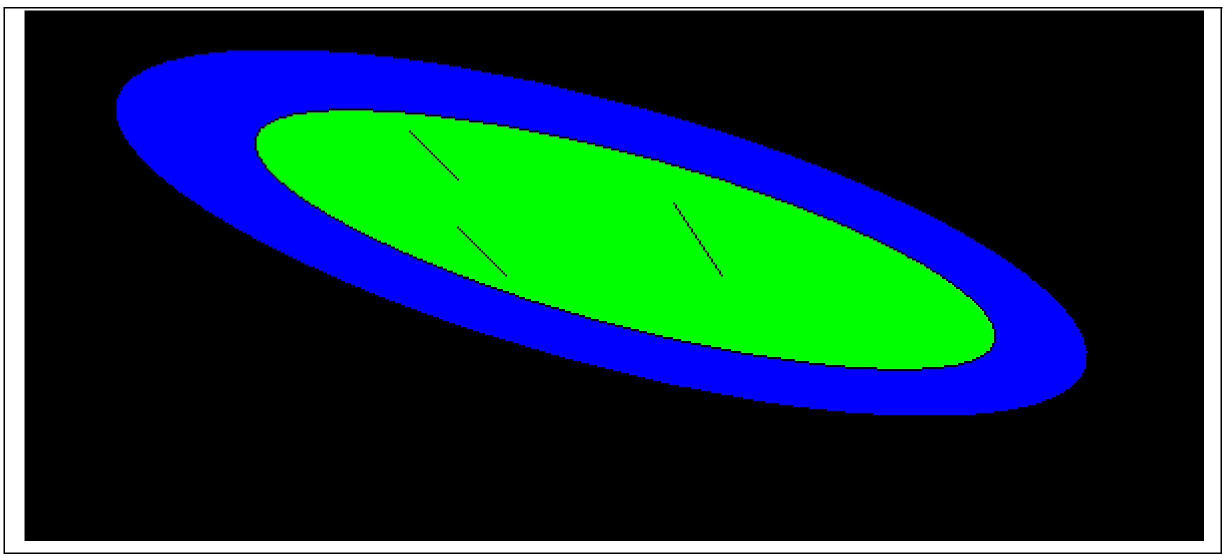
Figure 7: initial status of the dynamic model including the fluid saturation

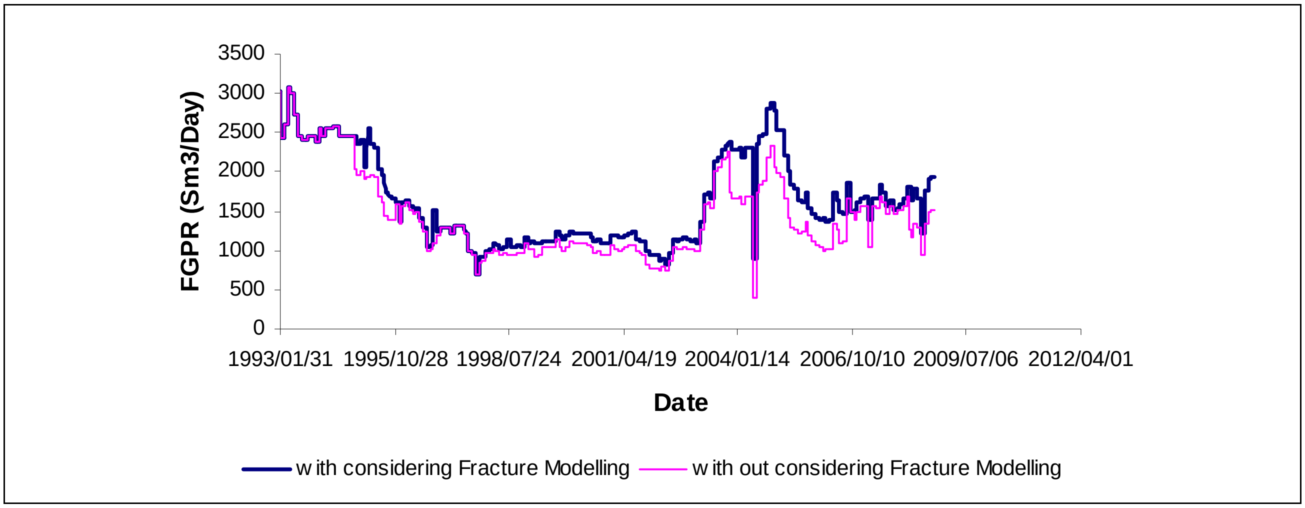

Figure 8: comparison of gas production rate history between 2 models

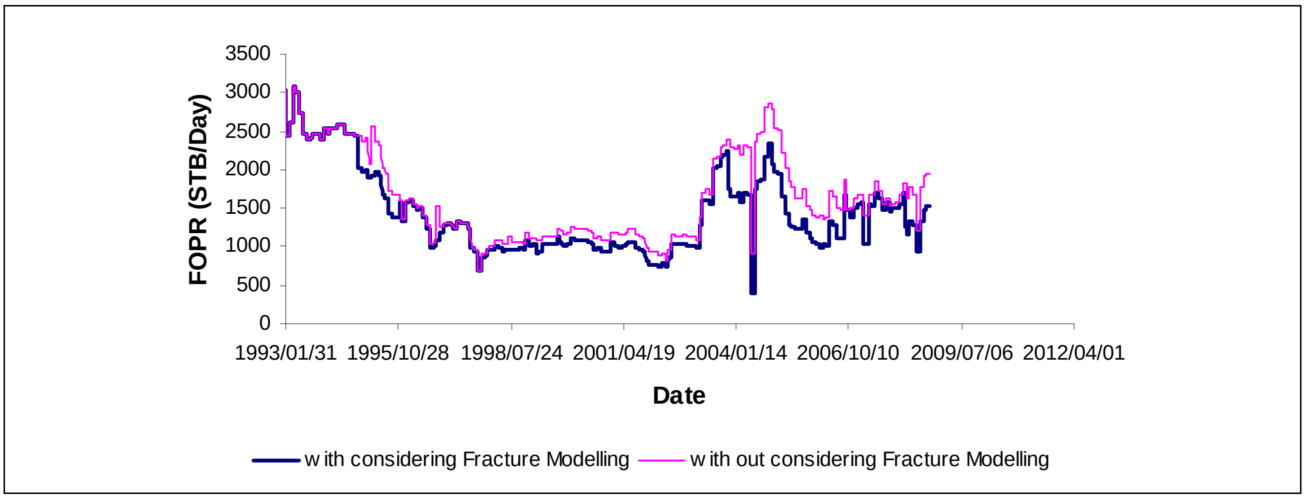

Figure 9: comparison of oil production rate history between 2 models

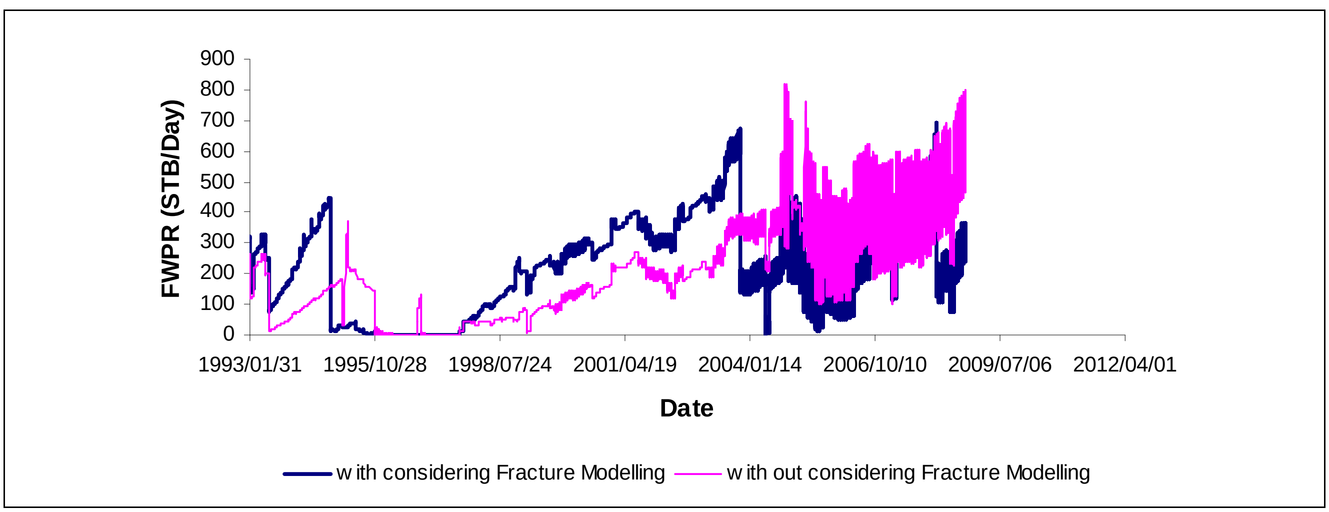

Figure 10: comparison of water production rate history between 2 models

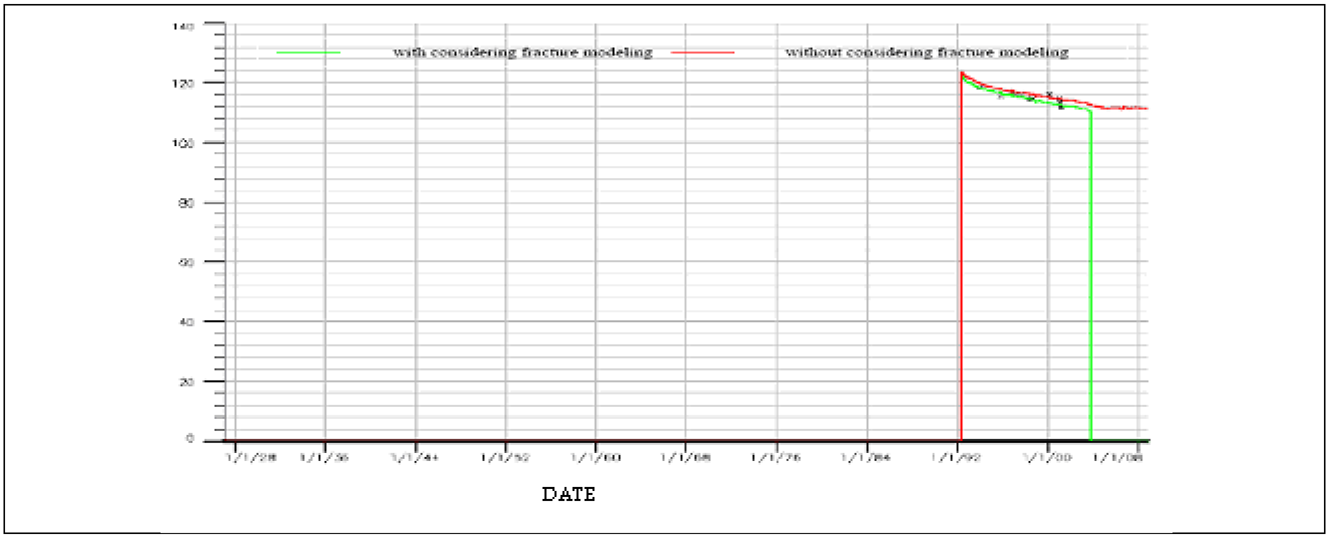

Figure 11: Comparison of well bottom hole pressure at one of production wells.

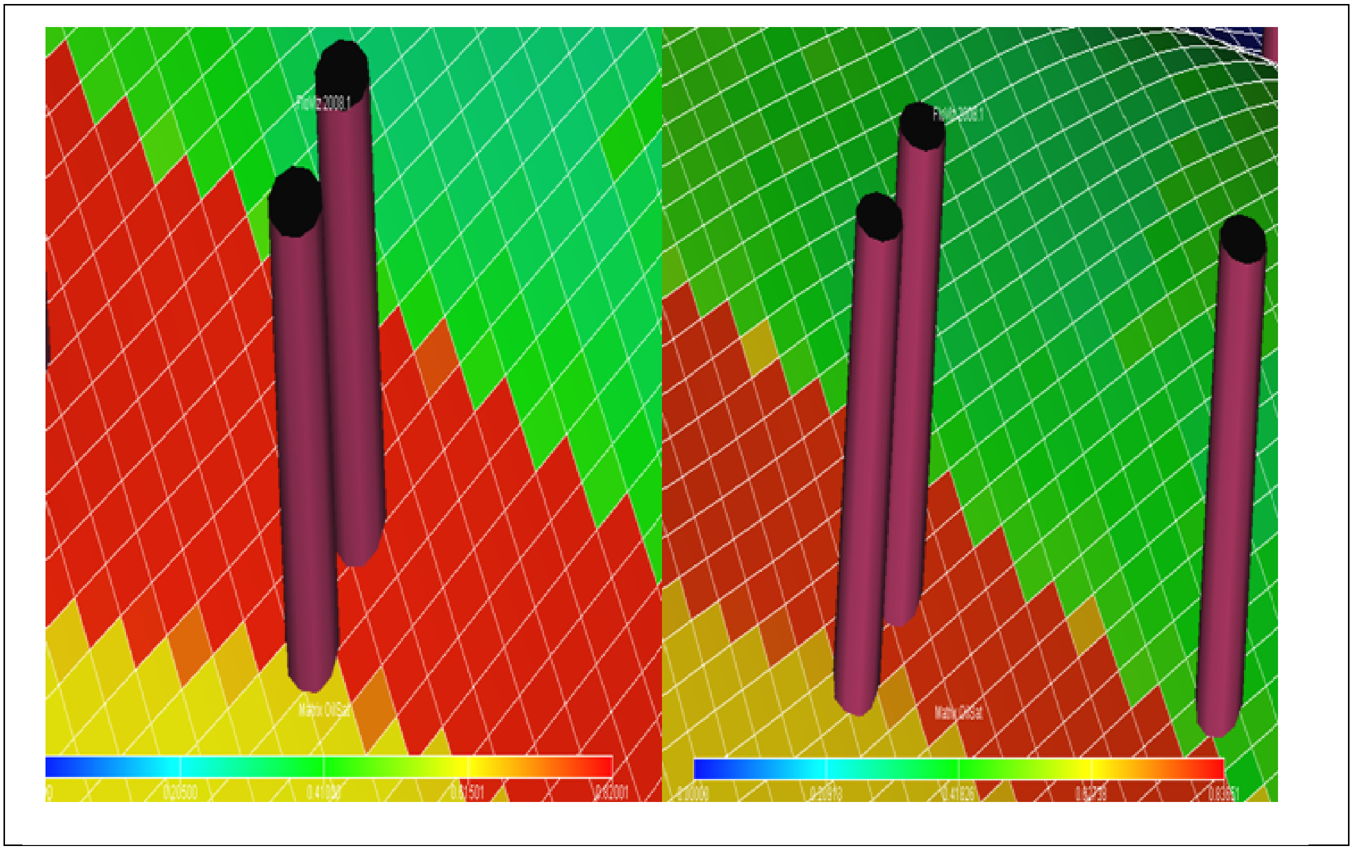
Figure 12: Comparison of oil rim thickness (oil saturation) at two models (the right one is with considering fracture modeling, the left one is without considering it)

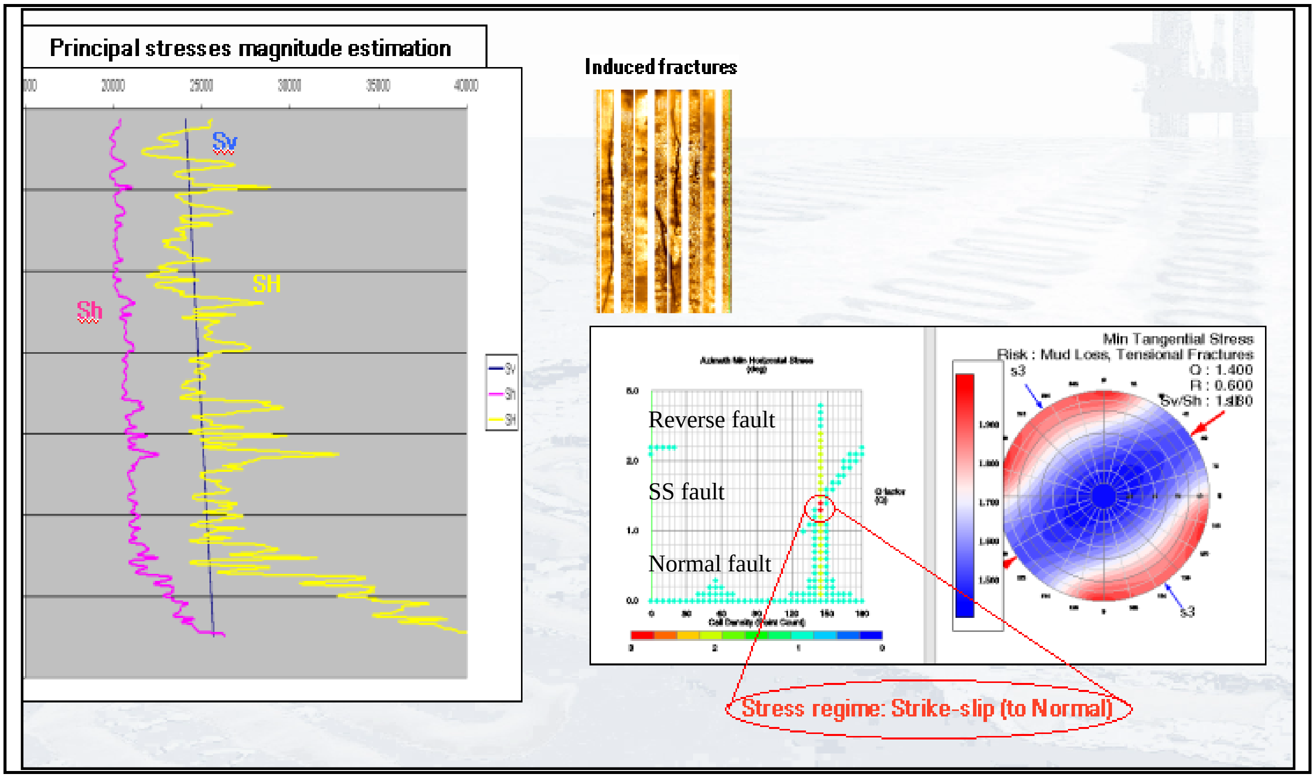

Figure 13: Stress regime determination and principal stress magnitudes across the reservoir.

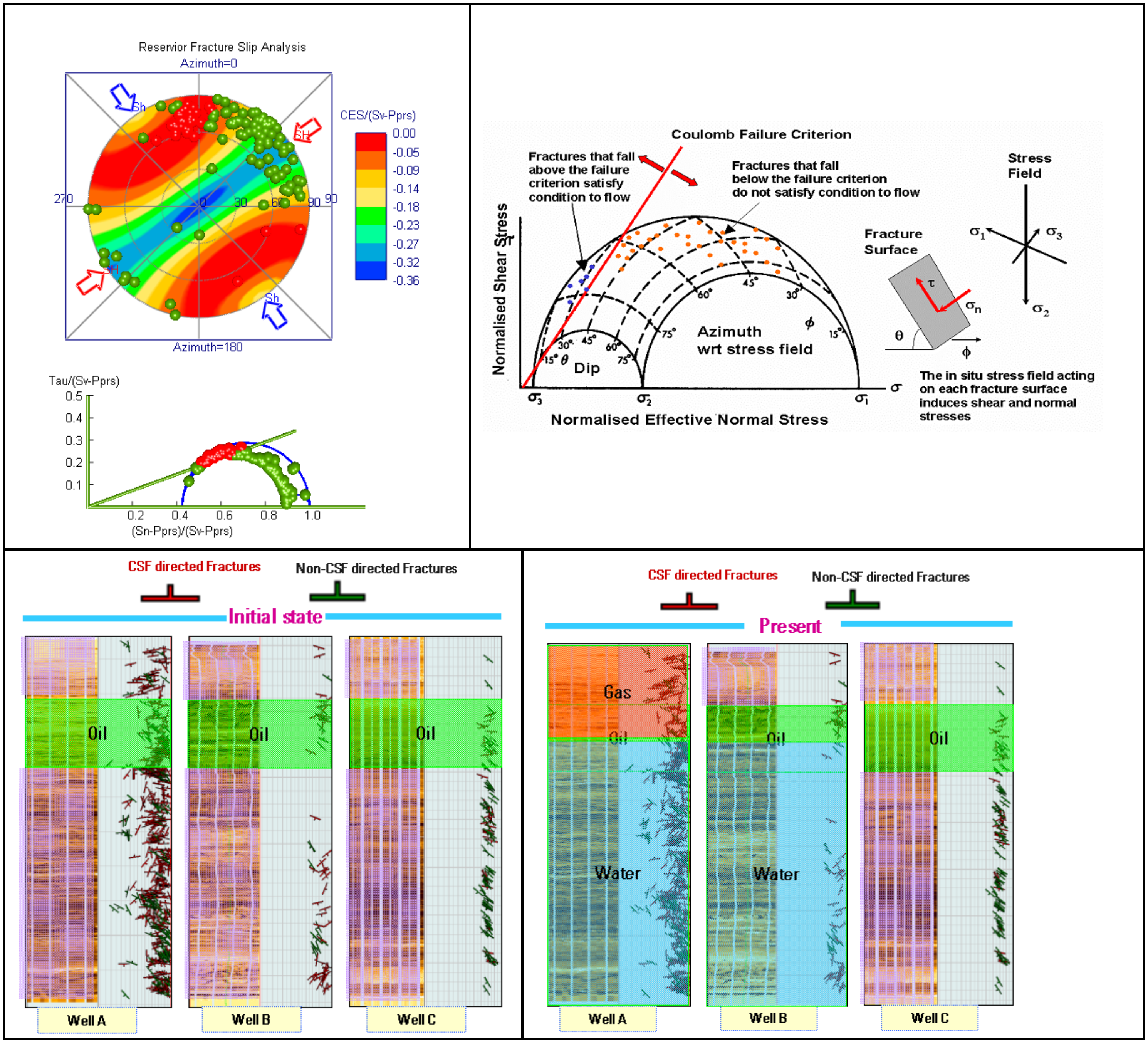

Figure 14: Above-right, principles of critically stressed fracturing (Barton & Zoback 1995), above-left, results of CSFA in well-B. Below-left, the initial state of production of wells A to C and below-right present state of production.